

Cite this: *J. Mater. Chem.*, 2012, **22**, 3671

www.rsc.org/materials

The application of graphene based materials for actuators

Yi Huang, Jiajie Liang and Yongsheng Chen*

Received 29th October 2011, Accepted 18th December 2011

DOI: 10.1039/c2jm15536b

Compared with traditional actuation materials, such as piezoelectric, ferroelectric and conducting polymer materials which suffered from low flexibility, high driving voltages and low energy efficiency, graphene exhibits outstanding mechanical, electrical, optical properties and chemical stability, which made it a good candidate for actuation materials. In this review, the recent progress in graphene based actuators induced by electric, electrochemical, optical and other stimulations are summarized.

Different actuation mechanisms and future developments are discussed. Graphene based materials, combining their many excellent properties, such as material abundance, super mechanical strength with excellent actuation performance, are expected to have great potential for the application in next generation actuators.

1. Introduction

An actuator is a mechanical device for moving or controlling a mechanism or system, which is operated by responding an appropriate external stimulus. Under such a controllable external stimulus, the actuator materials in the device undergo a reversible change in shape, volume, modulus, or some other mechanical property, corresponding to the conversion of other energy forms (stimulus) to mechanical energy. In other words,

actuators can also be treated as an energy conversion system which converts other external energy to mechanical energy. The stimulus can be electrical, thermal, pneumatic, or optical, depending on the actuation mechanism and energy supply. Actuators have been adopted in various applications, including medical devices,¹ switches, microrobotics,^{2,3} artificial muscle,⁴ shape memory materials, and many other smart structures. Commonly, actuator materials include inorganic materials, polymers, and carbon-based materials.⁵⁻⁷ Historically, a range of inorganic materials including shape memory alloys and piezoelectric ceramics have been evaluated as actuators.^{8,9} However, the requirement of high operating temperature and/or voltage restrict their range of applications. On the other hand, although polymer-based soft actuators including dielectric elastomers,

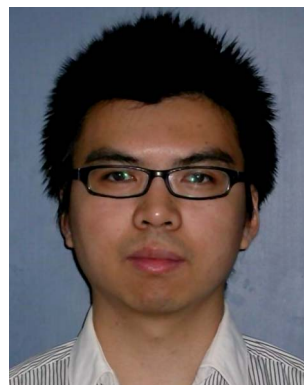
Key Laboratory of Functional Polymer Materials and the Centre of Nanoscale Science and Technology, Institute of Polymer Chemistry, College of Chemistry, Nankai University, Tianjin, 300071, China. E-mail: yihuang@nankai.edu.cn; leungjiajie@gmail.com; yschen99@nankai.edu.cn; Fax: +86 (22) 2349-9992; Tel: +86 (22) 2350-0693



Yi Huang

Prof. Yi Huang received his B.S. degree (1996) in Polymer Science and Engineering and Ph. D. degree (2001) in Materialogy from Sichuan University. He then spent two years as a postdoctoral fellow at Department of Chemical Engineering in Tsinghua University. From 2004, he has been an Associate Professor of Chemistry in Nankai University. His research interests focus on controlled synthesis and application of carbon nanomaterials (graphene and carbon nano-

tubes), polymer based nanocomposites and devices. He has published over 60 peer reviewed journal articles.



Jiajie Liang

Jiajie Liang received his B.S. from the Department of Chemistry at Nankai University (2006) and Ph.D. from the Institute of Polymer Chemistry at Nankai University under the direction of Prof. Yongsheng Chen (2011). Currently, he is a postdoctoral fellow in the group of Prof. Qibing Pei in the Department of Materials Science & Engineering at the University of California, Los Angeles. His research is focused on studying the applications of graphene-based materials

including graphene-based actuators, high-performance composites and electronic devices.

conjugated polymers and polymer gels have some advantages, such as flexibility, being lightweight, and having good optical transparency,^{10,11} their slow response, short life cycle, and low-energy conversion efficiency still limit the performance of polymer-based actuators. Moreover, the majority of these polymer based materials require post processing steps or assembly methods that are not compatible with conventional batch microfabrication steps.

Obviously, different actuator materials have different advantages and limitations.^{7,12–14} Hence, there are significant challenges in developing actuator materials for a large displacement and a rapid response at low voltages, as well as in developing a compatible fabrication method. Carbon-based materials, including carbon nanotubes, intend to offer actuation with very high stress output and efficiency at low voltage, but with low strain output. Due to their unique structure and many excellent properties, there have been reports that electromechanical actuators based on sheets of single-walled carbon nanotubes (SWNTs) can generate stresses higher than that of natural muscle and excellent strain at low applied voltages.^{5,15,16}

Graphene, as a stable 2D one atom layer material, exhibits many exciting properties which render it a possible competitive candidate for actuation materials.¹⁷ Its excellent electrical^{18,19} and thermal conductivity,²⁰ high surface area,²¹ super mechanical strength,^{22,23} high flexibility all are much demanded for a high performance actuator material. With this in mind, it is interesting to note that the studies for actuation using graphene are not as intensive as for many other areas, such as transparent electrode or supercapacitor using graphene. Possible reasons may include that such studies require very broad and interdisciplinary expertise, which really needs a joint effort from chemistry, physics and engineering science. Nevertheless, in only few years, great progress has been made in the actuation studies using graphene. In this feature article, we will summarize the progress made so far, and discuss the mechanism and propose our understanding for future works in this area. According to different stimuli, we will discuss the progress in three fields, that is, electrically, chemically and light stimulated actuation.

2. Electrically stimulated actuation

Electrically stimulated actuation is possibly the most common actuation, where the controllable electrical energy/signal is converted to mechanical energy/change. The first related work using graphene was reported by the McEuen group, where electromechanical resonators were demonstrated using suspended exfoliated graphene sheets.²⁴ The thinnest resonator (Fig. 1a) can be modulated by both electrical and light signal, with resonant frequency $f_0 = 70.5$ MHz for the single-layer graphene resonator (Fig. 1b). The resonant frequencies change with the thickness of the graphene sheets/layers, but all in the range of tens to hundreds of MHz. Also, the resonators give the highest modulus than any other resonators to date, greater than Si cantilevers and close to single-walled carbon nanotubes and diamond NEMS.²⁵ Importantly, in contrast to ultrathin Si cantilevers, the graphene resonators show no degradation in Young's modulus with decreasing thickness. This work was followed by a report about an array of doubly clamped nanomechanical graphene resonator using both electrical and light modulation.²⁶ The graphene array resonator was then patterned using standard photolithographic techniques and an oxygen plasma etch. The frequencies with different dimensional length of graphene sheets were studied, which are in the range of 55 KHz to 2.5 MHz (Fig. 1d). Again, later on, McEuen group reported an array of graphene resonators fabricated using chemical vapor deposition (CVD) growth followed by patterning and transfer.²⁷ The resonators were measured using both optical and electrical actuation and detection techniques, it was found that the resonance frequency is tunable with both electrostatic gate voltage and temperature, and quality factors improve dramatically with cooling, reaching values up to 9000 at 10 K. The results show that a CVD graphene resonator gives similar performance to that from exfoliated graphene. The frequencies are in the range of tens of MHz depending on the length and other factors of the graphene resonators.

In contrast with many conventional materials, graphene has a distinctive negative coefficient of thermal expansion (contraction upon heating).²⁸ Based on this, Zhu and *et al.* have designed and fabricated a biomorph graphene/epoxy hybrid biomorph actuator, where graphene acts as both the conducting and heating layer (Fig. 2a).²⁹ Due to the asymmetric thermo-mechanical response of graphene and epoxy layers, the actuation was achieved when electrical current was applied to the device, with high performance at low power input. For example, with an initial input of 1 V, the cantilever tip moved up 1 μm in 0.02 s ($\sim 50 \mu\text{m s}^{-1}$) and returned as fast as in ~ 0.1 s to its starting position ($\sim 13.3 \mu\text{m s}^{-1}$). A transparent dragonfly device based on it was fabricated and shown in Fig. 2b, where graphene is used for both actuation and structural support. The graphene-on-organic film actuator generates a flapping and bending movement that could be controlled by changing the frequency and the duration of the applied voltage.

A very recent and interesting report came from Jang's group.³⁰ They fabricated a graphene acoustic actuator prepared by inkjet printing, which can be used as an extremely thin and lightweight loudspeaker (Fig. 3). In this device, the actual actuation used the poly(vinylidene fluoride) (PVDF) thin film piezoelectric effect and printed graphene was used as the electrode. The graphene electrode was printed out on PVDF and then reduced using



Yongsheng Chen

Prof. Yongsheng Chen graduated from the University of Victoria with a Ph.D. degree in chemistry in 1997 and then joined University of Kentucky and UCLA for his postdoctoral studies from 1997 to 1999. Since 2003, he has been a Chair Professor at Nankai University. His main research interests include: 1) carbon-based nanomaterials, including carbon nanotubes and graphene; 2) organic and polymeric functional materials and 3) energy devices including OPV and supercapacitors, etc. He has published over 130 peer-reviewed papers and has over 20 patents.

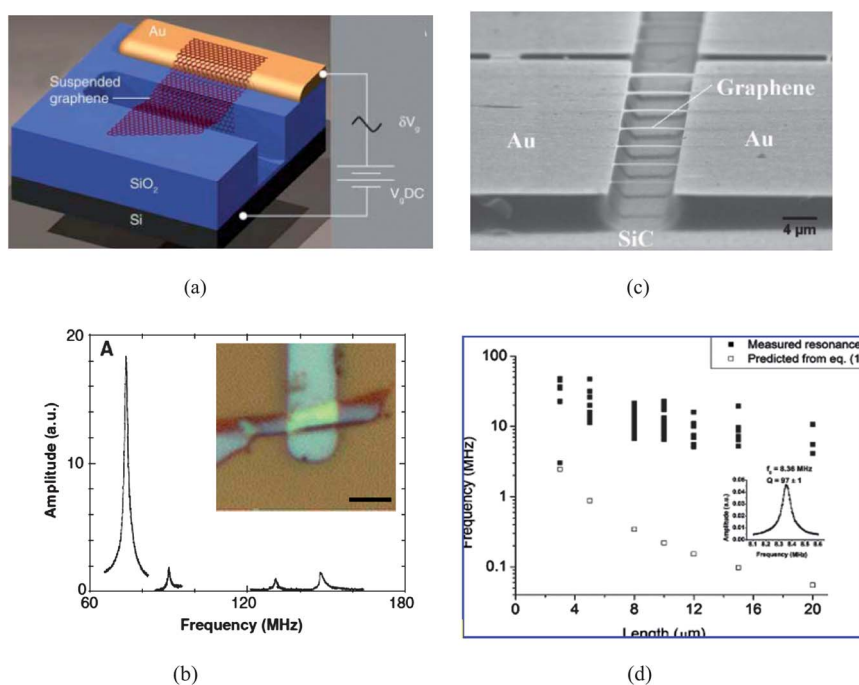


Fig. 1 (a) Schematic of a suspended graphene resonator. (b) Amplitude *versus* frequency for a 15 nm thick multilayer graphene resonator taken with optical drive. (Inset) An optical image of the resonator. Scale bar, 5 μm .²⁴ (c) Scanning electron microscope images of suspended epitaxial graphene (SEG). An array of doubly clamped nanomechanical graphene beams of length 8 μm and widths ranging from 0.5 to 3.5 μm . (d) Plot of resonances of devices of various lengths measured using laser interferometry. Inset shows measured resonance of a sample device with length 8 μm .²⁶ Reprinted with permission from the American Association for the Advancement of Science (copyright 2007) and the American Chemical Society (copyright 2009).

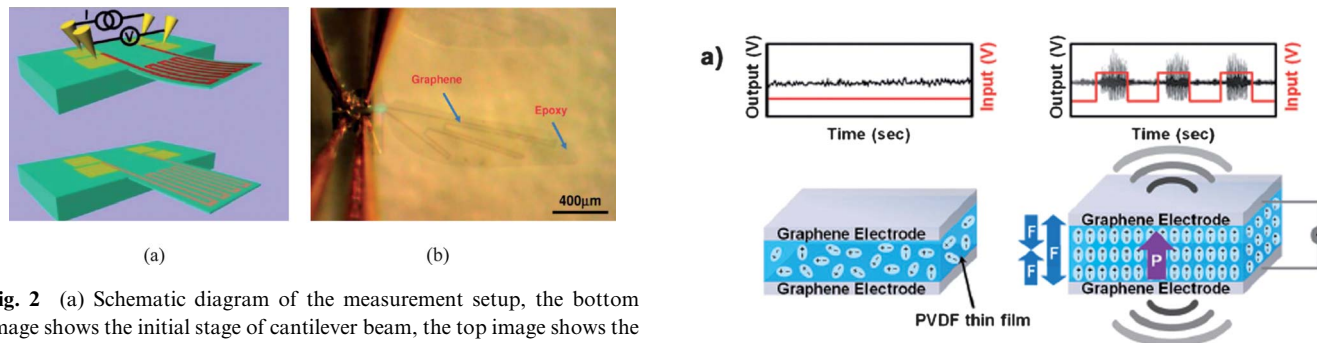


Fig. 2 (a) Schematic diagram of the measurement setup, the bottom image shows the initial stage of cantilever beam, the top image shows the upward deflection upon applying the electrical power. (b) Graphene-on-organic film which is in the form of a dragonfly wing.²⁹ Reprinted with permission from the American Chemical Society (copyright 2011).

hydrazine vapor at 90 °C under vacuum. The actuator speaker has effective response in the range of 40 Hz to 20 KHz. In addition, the acoustic actuators with a transparent and flexible graphene electrode had higher responses over all frequencies than those with a commercial PEDOT:PSS electrode. There was an earlier report for a transparent, flexible, stretchable, and magnet-free speaker, where carbon nanotubes work directly as the actuation material. It was found that very thin carbon nanotube films, when fed by sound frequency electric currents, could emit loud sounds due to the thermoacoustic effect.³¹ This is a truly excellent demonstration for the nanotube electrical actuation. The ultra small heat capacity per unit area of carbon nanotube thin films leads to a wide frequency response range and a high sound pressure level.



Fig. 3 (a) Schematic illustration and (b) photograph of a PVDF-based thin film acoustic actuator using flexible and transparent graphene electrodes. P and F mean polarization and force of the acoustic actuator, respectively.³⁰ Reprinted with permission from the Royal Society of Chemistry (copyright 2011).

Wang *et al.* prepared composite fibers of graphene and CNTs with PVA (poly(vinyl alcohol)) by a coagulation spinning technique.³² The co-existence of graphene and CNTs make the fibers have better synergetic conductivity and tensile strength than the fibers with either graphene or CNTs due to the mutual dispersion effect of these two carbon allotrope graphene and CNT. These composite fibers showed excellent electromechanical performance in air. When a sine voltage wave is applied, that the actuated displacement vibrates exactly in line with the input voltage and hence perfect sine curves with the same frequencies are obtained as shown in Fig. 4. Note that the displacement was always in the same direction, independent of the direction of the applied voltage. This indicates that the actuation mechanism is an electrothermal one. When an alternating current passed through the fiber, periodic heating took place, which resulted in cycling thermal expansion and contraction. The rapid response of these fibers is mainly attributed to their both high conductivity and excellent thermal conductivity.

A pristine graphene oxide (GO) paper, prepared using GO solution without any post treatment, was studied by Oh and *et al.* for its electromechanical actuation.³³ They found that the GO paper exhibited up to 1.6% reversible contraction when electrically heated at ambient conditions, with energy density of 40 J kg⁻¹, which is similar to that of natural muscle. Using *in situ* X-ray diffraction measurement, it was found that the dimensional changes were associated with reversible adsorption/desorption of water molecules between graphene layers in the GO paper.

Cao *et al.* have made a composite of GO with Nafion using a simple solution mixing and studied the actuation performance of a cantilevered actuation system made of the membrane of this composite.³⁴ They found that the GO composite has much better performance than that of the pure Nafion membrane, in terms of both displacement and blocking force. This is due to both the better dispersion and improved conductivity. The blocking force of membrane containing 10 wt% GO gave the highest blocking force, about four times that of pure Nafion, which is better than that for the CNT/Nafion actuator.³⁵

Great progress has been made in graphene based electromechanical actuators. Graphene, graphene oxide and graphene-based composite materials have been used to convert electrical energy to mechanical energy. But the mechanism of this actuation behavior has not been fully understood. More detailed

research work need to be done to reveal the energy conversion and shape change process.

3. Electrochemically stimulated actuation

Electrochemically stimulated actuation involves the actuation caused by ion-doping of actuator materials under electrochemical conditions. Generally, actuators consist of a bilayer architecture, where the two materials on the different side of the actuators behavior differently under same electrochemical conditions, and this difference causes the actuation. Recently, Qu and co-workers came up with a very different approach with only one material, graphene, and designed and prepared a unimorph electrochemical actuator based on a monolithic graphene film with asymmetrically modified surfaces.³⁶ They first prepared the normal graphene film using filtration as usual, but then treated the two sides of the film differently. One side was treated with hexane plasma, and the other side was treated with O₂ plasma. These different treatments made the two surfaces exhibit very different properties. For example, the side which underwent O₂ plasma treatment shows hydrophilic and enhanced area capacitance (2.83 mF cm⁻²). On contrary, the side which underwent hexane plasma treatment shows much less hydrophilic with a CA of only 0.05 mF cm⁻². These differences make them show actuation under electrochemical conditions such as in aqueous NaClO₄ solution. For example, when scanning within the potential region of ±1.2 V, the graphene strip showed a deflection of up to about 15 mm at the strip tip, which reversed on reversal of the applied potential (Fig. 5a). As for control, the untreated graphene film or the films treated the same for both sides do not show the actuation. It was proposed that the graphene actuator works mainly *via* the non-Faradaic electrical charging/discharging analogous to the CNT-based actuators.⁵ Because of the asymmetry of the graphene film, the difference in electrochemically induced charge injections into the plasma/graphene interfaces at the two opposite sides result in the deformation of the graphene film, and thus the actuation. The authors also investigated the length changes of graphene strips treated solely with hexane and oxygen plasma under applied square wave potentials. Similar to the case of a CNT actuator,⁵ the electron injection into a graphene sheet electrode could cause an expansion, while a contraction occurred for the hole injection

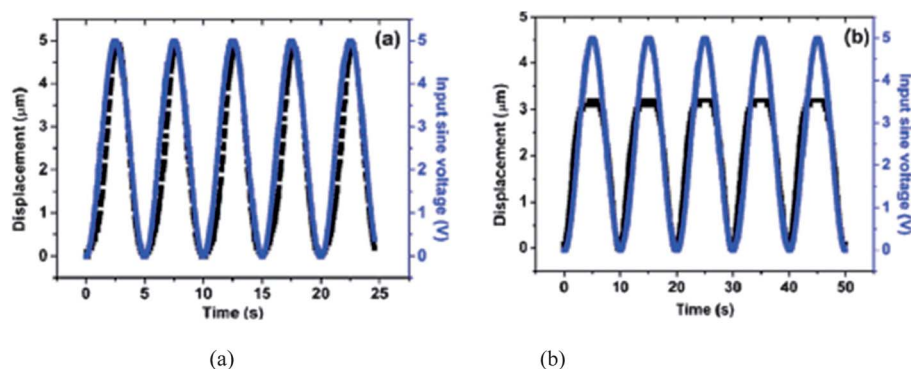


Fig. 4 Displacement vibration of SWCNT-GO fibers under input sine voltage (a) 0–5 V, 0.2 Hz; (b) 0–5 V, 0.1 Hz.³² Reprinted with permission from the Royal Society of Chemistry (copyright 2011).

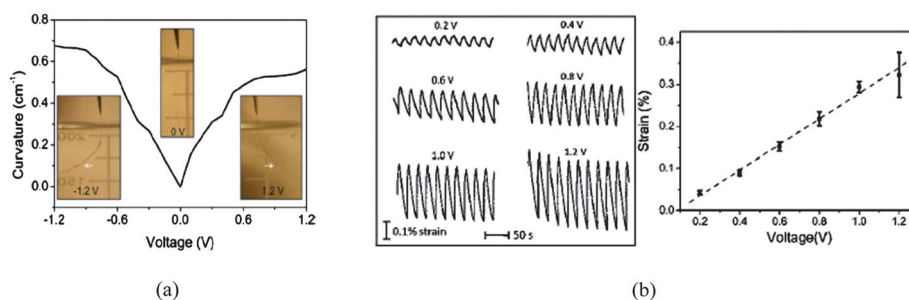


Fig. 5 (a) Curvature change of an Asy-modified graphene strip as a function of applied CV potential within ± 1.2 V. Insets show the status of the graphene strip at -1.2 , 0 , and 1.2 V, respectively.³⁶ (b) The strain response of a graphene actuator at different applied square wave potentials, and the corresponding strain changes as a function of applied square wave voltages with a frequency of 0.05 Hz (4 kPa load).³⁷ Reprinted with permission from the American Chemical Society (copyright 2010) and the Royal Society of Chemistry (copyright 2011).

process. In this case, the oxygen plasma treated graphene strip displayed a rhythmic length change of up to 0.2% in response to the potential change, while the hexane plasma treated one exhibited a noise-like fluctuation.

With symmetrical graphene films, Qu and *et al.* later reported that the actuator made of such graphene films showed superior strain response (0.85%),³⁷ far exceeding that for CNT based actuators. The actuation measurement was carried using a cantilever setup in NaClO_4 aqueous solution. The strain response of graphene film in strip type remained stable under the measurable loading range, and the tolerant load for the graphene film in scroll type could be up to 6.1 MPa with only slight decrease of the strain response. The cyclic voltammograms of the graphene film is shown in Fig. 5b, where the high strain changes of graphene strips were clearly demonstrated. There is a uniform strain response with the square wave input (Fig. 5b). The strain of the graphene strip closely follows the applied square wave potential. The change of strain increases linearly with the increase of applied voltage. At an applied square wave potential of 1.2 V with a frequency of 0.05 Hz, the strain can reach 0.35% , much higher than that generated by single-walled and multi-walled CNTs ($\sim 0.2\%$).³⁸ Also, durability measurement for several hours has verified the response stability of graphene films. The higher strain for graphene actuator compared that made of CNTs is due to the factor that graphene is more planar structure while CNTs have a more tubular structure. This gives graphene more freedom to expand when charged compared with CNTs.

Oh and co-authors further studied the electrochemical actuation of graphene–Nafion composite, which was made by solution mixing of reduced GO with Nafion.³⁹ The cast membrane of the solution, after annealed at 140 °C for 2 h, was used to measure the actuation.

The tensile strength of the composite membrane was significantly improved up to 200% within a 1.0 wt% graphene loading, and Young's modulus was more than two times of that of pristine Nafion membrane. The proton conductivity and the water-uptake ratio were also greatly improved. The composite materials show much improved actuation performance compared with of the Nafion pristine material. For example, the tip displacement of 1.0 wt% of graphene-reinforced actuator is almost twice that of the recast Nafion-based ionic polymer-metal composite (IPMC) actuator. (Fig. 6) The maximum harmonic response of the graphene (1.0%)-reinforced composite actuators

was about three times of that of Nafion actuator. Similarly, in many other reports, the displacement decreases with increasing frequency. A low blocking force of the electro-active IPMC actuator is a critical problem to be improved for realistic application. The blocking force is defined as a required force at the tip of a bending actuator when the tip position is kept fixed, *i.e.* identically zero deflection. In this case, the blocking force of the graphene reinforced Nafion actuator was about three times as big as that of the Nafion actuator. Also, current–voltage tests and subsequent efficiency analysis showed that specific electromechanical efficiency of graphene-reinforced actuators is almost twice than that of recast Nafion.

When prepared bulk (composite) materials of graphene, such as from GO, one important issue is to prevent the re-stacking of graphene sheets during the reduction process of GO. To achieve this, either functionalization of graphene or adding a spacer between the graphene sheets can be used.^{40–43} At the same time, other functions could be added by functionalization or by using spacer materials. Using the spacer approach, we have made a composite material of graphene with magnetic Fe_3O_4 nanoparticles.⁴⁴ Flexible and strong paper-like materials could be obtained by the simple filtration of such composite material solutions. Electromechanical actuation was studied for the pristine graphene paper, and composite papers in 1 M NaCl solution.⁴⁵ Due to the intercalation of Fe_3O_4 particles between the graphene sheets, the access of electrolyte ions is much easier and more efficient in the case of composite actuator as shown in Fig. 7. Indeed, the composite actuators show much improved actuation performance. For example, the pristine graphene paper, annealed at 400 °C, shown actuation strain about 0.064% , while the magnetic graphene papers presented a higher actuation strain (0.1%) than the pristine graphene papers. Based on our experimental results, we predict that the maximum intrinsic strain for a single graphene sheet or graphene papers composed of non-restacked graphene sheets is as large as 1.2% or even higher.

4. Actuation of graphene with other stimulus

In addition to electrical and electrochemical stimulus discussed above, there are a few reports using other stimulus for the actuation of graphene-based actuators. Optical-induced actuators, compared to the actuators driven by other stimuli, offers an

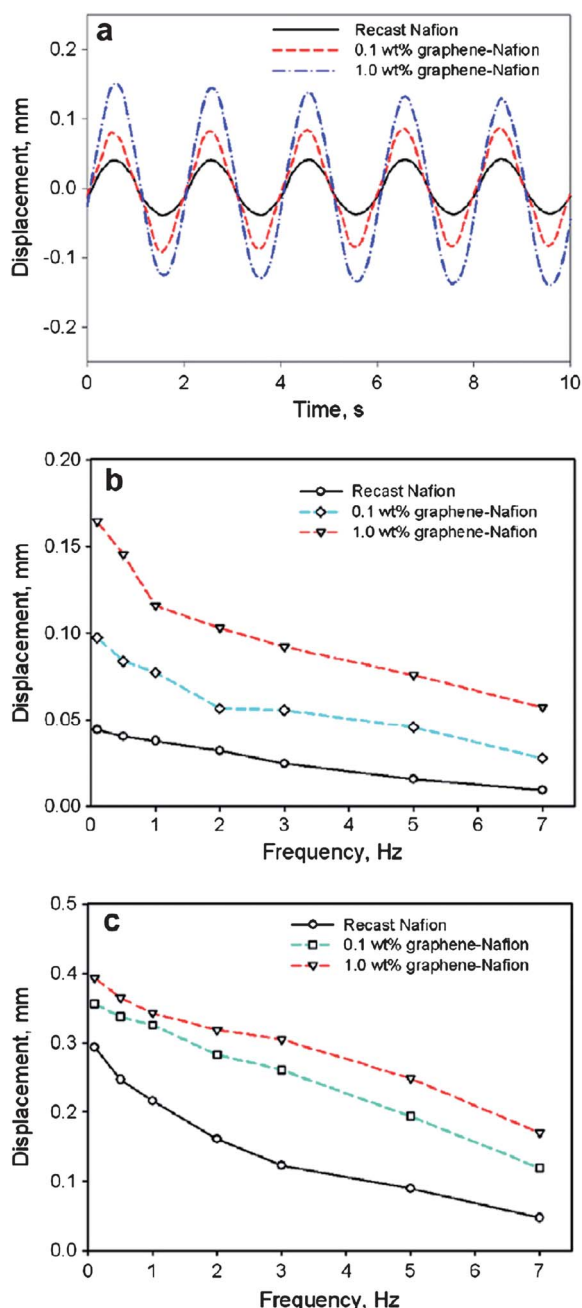


Fig. 6 Actuated tip displacements under sinusoidal electrical inputs of $0.5 \times \sin(2\pi \times 0.5 \times t)$ (a), tip-displacement histories in the harmonic responses at the excitation voltages of 0.5 V (b) and 1.5 V (c) according to applied frequencies.³⁹ Reprinted with permission from the Elsevier Limited (copyright 2011).

attractive way to control actuation remotely, which brings excellent advantages such as wireless actuation, remote control, and high-level integrity.⁴⁶ Significant progress has been made recently in the development for polymer-based optical-triggered actuator materials because of the polymer material's light weight, good processability, and low cost and particularly because it has stroke, force, and efficiency similar to that of human muscles. These advantages make the optical-triggered polymeric actuators promising for a variety of applications especially in the field of

medical devices where triggers other than heat or electricity are highly desirable.⁴⁷ Currently, two types of light-triggered polymeric actuators have been reported including pure polymers^{47–49} and polymer composites.^{47,50–53} In either of these cases, these polymeric materials have to be equipped with photoactive functional groups or fillers. That is, both of these two types of actuator materials need to consist of two components on the intra or inter molecule level: “molecular switch” and “energy transfer” units, where the former works as the mechanical deformation (molecular switch) unit and the later acts as the trigger (energy transfer) unit to transfer the external light energy to the “molecular switch” unit.⁴⁹ Thermoplastic polyurethane (TPU), which possesses the ability to store and efficiently recover large strains by application of prearranged thermal stimuli due to its two-phase structure: a thermally reversible phase responsible for fixing a transient shape and a frozen phase responsible for recovering the original shape^{50,54–57} is one of the widely used polymeric thermally-induced actuator materials. Unfortunately, its high transparency makes it show no light-induced actuation.⁵⁰ When it is combined with carbon nanotubes (CNTs), the nanocomposite show excellent remote, rapid and high energy infrared-induced actuation behavior, along with remarkable enhancement of mechanical performance.⁵⁰ However, the inherent bundling of carbon nanotubes, their intrinsic impurities from catalysts and amorphous carbon, poor dispersibility, as well as high cost have limited the potential of these composite materials. In many aspects, graphene may rival or even surpass carbon nanotubes.^{18,19,58–64} Thus, nanocomposites utilizing graphene materials as nanofillers are offering opportunities to impart unprecedented enhancing mechanical and thermal properties to polymers at very low loadings.⁶³ Moreover, the perfect sp^2 carbon-network structures of the graphene materials ensure them to have excellent thermal conductivity and IR response.^{20,65,66} Given these combined and unique properties of graphene materials as well as the thermally-active characteristic of TPU, it is thus expected that graphene/TPU nanocomposites could work as photoactive “energy transfer” materials and TPU can act as “molecular switch” units, an actuator could be built with salient IR-triggered actuation behavior. Based on these thoughts, we have developed graphene/TPU nanocomposite actuators with three kinds of graphene fillers: sulfonated functionalized graphene sheets (sulfonated-graphene),⁶⁷ isocyanate treated graphene oxide⁶⁸ and reduced graphene-based sheets.⁶⁹ Indeed, sulfonated-graphene, which is prepared with pre-reduction of graphene oxide followed by a diazonium reaction for the attachment of SO_3H group and then a postreduction with hydrazine,⁶⁷ shows the best IR-absorption properties in these three fillers and a much improved conductivity⁶⁷ compared with the pristine GO material. The nanocomposite actuator with 1 wt % loading of sulfonated-graphene exhibits repeatable infrared-triggered actuation performance which can strikingly contract and lift a 21.6 g weight 3.1 cm with 0.21 N of force on exposure to infrared light and demonstrate estimated energy densities of over 0.33 J g^{-1} (Fig. 8).⁷⁰ Some cases can even reach as high as 0.40 J g^{-1} . We believed that this excellent actuation performance is mainly attributed to the following reason: the sulfonated-graphene, which is provided with relative perfect aromatic network and stable dispersion state in polymer matrix, can efficiently absorb and transform IR light into thermal energy and

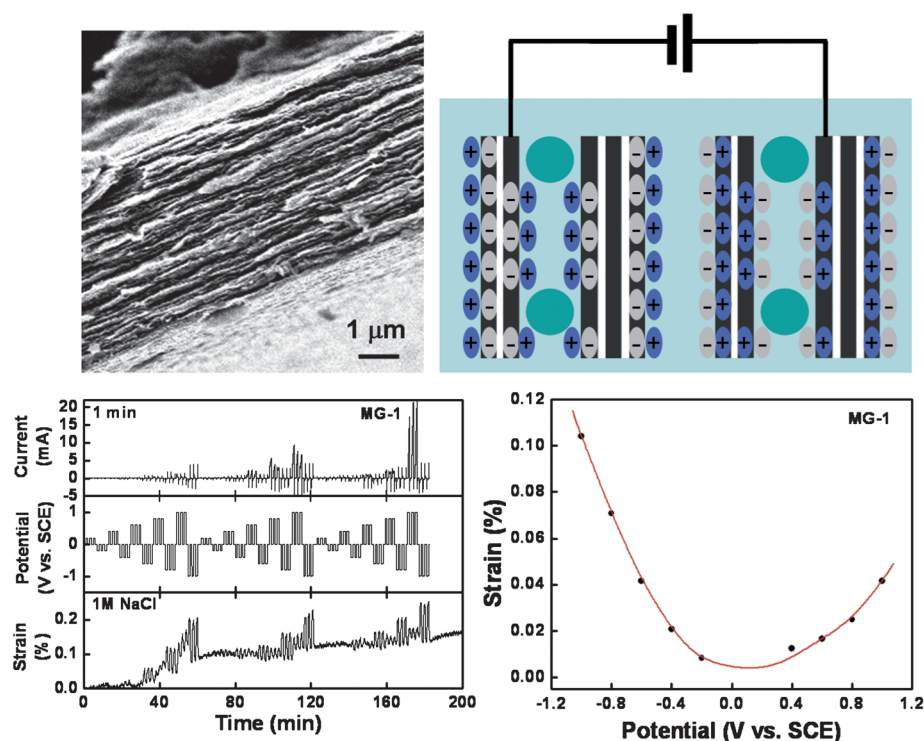


Fig. 7 Electromechanical actuators based on graphene and graphene/ Fe_3O_4 hybrid paper.⁴⁵ Reprinted with permission from John Wiley and Sons (copyright 2011).

can serve as a nanoscale heater and energy-transfer unit through its homogeneous network to heat the TPU matrix uniformly and rapidly; the absorbed thermal energy then raises the internal temperature, melting the strain-induced TPU polymer crystallites, which act as physical cross-links that secure the deformed shape, and remotely triggers the shape recovery.

Ruoff *et al.* have prepared a flexible bilayer “paper” composed of a layer of crisscrossed multi-walled CNTs (MWCNTs) and a layer of GO using solution filtration.⁷¹ The layer of graphene is electrically insulating while that of MWCNT layer was electrically conductive. This asymmetry could open the possibility of

applications in wrapping and as storage materials. Note that the OH and COOH groups on the GO sheet make it rather sensitive to humidity, this is different from CNTs. Thus, the actuation of the bilayer paper samples as a function of the relative humidity was investigated at room temperature. The bilayer papers were actuated by chemical environment—they curled depending on the relative humidity (Fig. 9). For example, at low relative humidity (12%) the bilayer paper rolled up with the MWCNT side facing outward (Fig. 9a). As the relative humidity exceeded $\sim 60\%$, the bilayer paper started to curl in the opposite direction, with the MWCNT side facing in and the graphene oxide side facing out

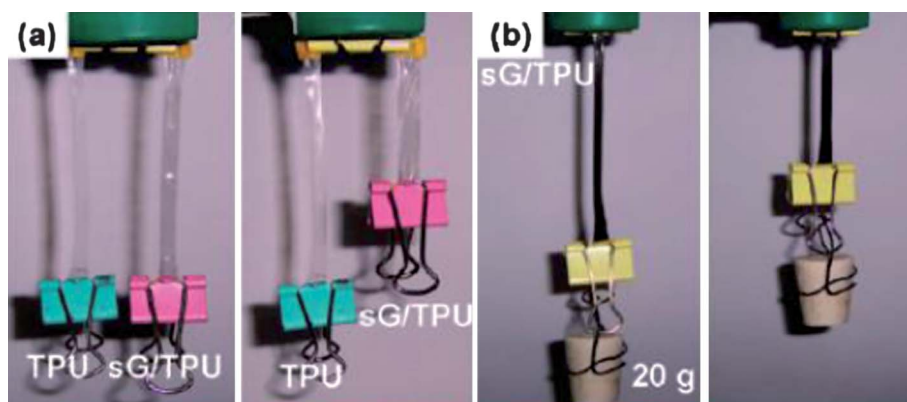


Fig. 8 Optical images of IR actuation for graphene-based nanocomposites. (a) Comparison of shape recovery before (left) and after (right) remotely actuated by infrared light. Pure TPU did not recover; in contrast, 0.1 wt% sulfonated-graphene/TPU nanocomposites (sG/TPU) (30 mm \times 5 mm \times 0.05 mm) contracted after actuated by infrared irradiation. (b) The 1 wt% sulfonated-graphene/TPU film contracted and lifted a 21.6 g weight 3.1 cm with 0.211 N of force on exposure to infrared light and demonstrated an estimated energy density of 0.33 J g^{-1} .⁷⁰ Reprinted with permission from the American Chemical Society (copyright 2009).

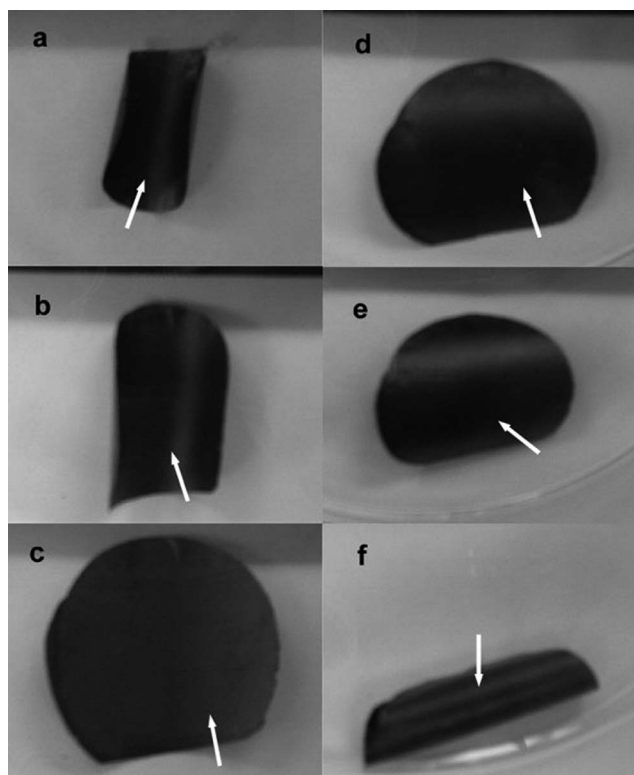


Fig. 9 Actuation of the bilayer paper sample as a function of relative humidity (%). (a) 12, (b) 25, (c) 49, (d) 61, (e) 70, and (f) 90. White-arrowed side: surface of graphene oxide layer.⁷¹ Reprinted with permission from the John Wiley and Sons (copyright 2010).

(Fig. 9d, e). The papers show similar behavior with different temperature. It is believed that the actuation of the bilayer paper might be induced by this different amount of interlamellar water of both layers depending on the relative humidity or temperature.

5. Conclusions

The booming of studies on graphene has only taken place in seven years, but in such a short period of time, we have witnessed many dramatic and unprecedented results for graphene. This includes many excellent results on the actuation studies using graphene. Significant results have been achieved for the actuation by electrical, chemical, light and other stimulus. But compared with other areas of graphene, the studies of actuation using graphene materials seem far behind. This is even more obvious if we consider the combination and collective advantages of graphene in mechanical, electrical, chemical stability and optical properties. So there are many and exciting opportunities ahead in this field. Although the studies on electromechanical actuation using graphene attract most attention, still much more work is needed to understand the actuation mechanism and improve the fabrication of actuators for more practical, large scale and flexible devices and shall offer many exciting results. In the meantime, actuation by other stimulus, such as light or chemical stimulation may produce more exciting results when the synergic performance of graphene is achieved. There are still some challenges waiting for us, such as increasing the actuation

strain, energy conversion efficiency and life cycle. With more progress in the material optimization and novel device design, we believe that graphene-based actuators will lead to a wide range of applications, including artificial muscles, robots, micro electro mechanical systems and so on.

Acknowledgements

The authors gratefully acknowledge financial support from the MOST (Grants 2012CB933401 and 2011CB932602) and NSFC (Grants 50902073, 50903044 and 50933003).

References

- 1 J. H. Jeon, T. H. Cheng and I. K. Oh, *Sens. Actuators, A*, 2010, **158**, 300.
- 2 J. H. Jeon and I. K. Oh, *Thin Solid Films*, 2009, **517**, 5288.
- 3 S. W. Yeom and I. K. Oh, *Smart Mater. Struct.*, 2009, **18**, 085002.
- 4 J. Lu, S. G. Kim, S. Lee and I. K. Oh, *Adv. Funct. Mater.*, 2008, **18**, 1290.
- 5 R. H. Baughman, C. X. Cui, A. A. Zakhidov, Z. Iqbal, J. N. Barisci, G. M. Spinks, G. G. Wallace, A. Mazzoldi, D. De Rossi, A. G. Rinzler, O. Jaschinski, S. Roth and M. Kertesz, *Science*, 1999, **284**, 1340.
- 6 V. Palmre, E. Lust, A. Janes, M. Koel, A. L. Peikolainen, J. Torop, U. Johanson and A. Aabloo, *J. Mater. Chem.*, 2011, **21**, 2577.
- 7 M. Tahhan, V. T. Truong, G. M. Spinks and G. G. Wallace, *Smart Mater. Struct.*, 2003, **12**, 626.
- 8 K. Byungkyu, L. Sunghak, H. P. Jong and P. Jong-Oh, *IEEE/ASME Trans. Mechatron.*, 2005, **10**, 77.
- 9 C. R. de Lima, S. L. Vatanabe, A. Choi, P. H. Nakasone, R. F. Pires and E. C. Nelli Silva, *Sens. Actuators, A*, 2009, **152**, 110.
- 10 S. Maeda, Y. Hara, T. Sakai, R. Yoshida and S. Hashimoto, *Adv. Mater.*, 2007, **19**, 3480.
- 11 R. H. Baughman, *Synth. Met.*, 1996, **78**, 339.
- 12 T. Mirfakhrai, J. D. W. Madden and R. H. Baughman, *Mater. Today*, 2007, **10**, 30.
- 13 C. Liu, H. Qin and P. T. Mather, *J. Mater. Chem.*, 2007, **17**, 1543.
- 14 C. Li, E. T. Thostenson and T. W. Chou, *Compos. Sci. Technol.*, 2008, **68**, 1227.
- 15 T. Mirfakhrai, J. Oh, M. Kozlov, E. C. W. Fok, M. Zhang, S. Fang, R. H. Baughman and J. D. W. Madden, *Smart Mater. Struct.*, 2007, **16**, S243.
- 16 T. Mirfakhrai, J. Oh, M. Kozlov, S. Fang, M. Zhang, R. H. Baughman and J. D. Madden, *Adv. Sci. Technol.*, 2008, **61**, 65.
- 17 A. K. Geim and K. S. Novoselov, *Nat. Mater.*, 2007, **6**, 183.
- 18 K. S. Novoselov, A. K. Geim, S. V. Morozov, D. Jiang, Y. Zhang, S. V. Dubonos, I. V. Grigorieva and A. A. Firsov, *Science*, 2004, **306**, 666.
- 19 P. Avouris, Z. H. Chen and V. Perebeinos, *Nat. Nanotechnol.*, 2007, **2**, 605.
- 20 A. A. Balandin, S. Ghosh, W. Z. Bao, I. Calizo, D. Teweldebrhan, F. Miao and C. N. Lau, *Nano Lett.*, 2008, **8**, 902.
- 21 J. L. Xia, F. Chen, J. H. Li and N. J. Tao, *Nat. Nanotechnol.*, 2009, **4**, 505.
- 22 C. Lee, X. D. Wei, J. W. Kysar and J. Hone, *Science*, 2008, **321**, 385.
- 23 T. J. Booth, P. Blake, R. R. Nair, D. Jiang, E. W. Hill, U. Bangert, A. Bleloch, M. Gass, K. S. Novoselov, M. I. Katsnelson and A. K. Geim, *Nano Lett.*, 2008, **8**, 2442.
- 24 J. S. Bunch, A. M. van der Zande, S. S. Verbridge, I. W. Frank, D. M. Tanenbaum, J. M. Parpia, H. G. Craighead and P. L. McEuen, *Science*, 2007, **315**, 490.
- 25 V. Sazonova, Y. Yaish, H. Ustunel, D. Roundy, T. A. Arias and P. L. McEuen, *Nature*, 2004, **431**, 284.
- 26 S. Shivaraman, R. A. Barton, X. Yu, J. Alden, L. Herman, M. V. S. Chandrashekar, J. Park, P. L. McEuen, J. M. Parpia, H. G. Craighead and M. G. Spencer, *Nano Lett.*, 2009, **9**, 3100.
- 27 A. M. van der Zande, R. A. Barton, J. S. Alden, C. S. Ruiz-Vargas, W. S. Whitney, P. H. Q. Pham, J. Park, J. M. Parpia, H. G. Craighead and P. L. McEuen, *Nano Lett.*, 2010, **10**, 4869.
- 28 W. Bao, F. Miao, Z. Chen, H. Zhang, W. Jang, C. Dames and C. N. Lau, *Nat. Nanotechnol.*, 2009, **4**, 562.

- 29 S. E. Zhu, R. Shabani, J. Rho, Y. Kim, B. H. Hong, J. H. Ahn and H. J. Cho, *Nano Lett.*, 2011, **11**, 977.
- 30 K. Y. Shin, J. Y. Hong and J. Jang, *Chem. Commun.*, 2011, **47**, 8527.
- 31 L. Xiao, Z. Chen, C. Feng, L. Liu, Z. Q. Bai, Y. Wang, L. Qian, Y. Zhang, Q. Li, K. Jiang and S. Fan, *Nano Lett.*, 2008, **8**, 4539.
- 32 R. R. Wang, J. Sun, L. Gao, C. H. Xu and J. Zhang, *Chem. Commun.*, 2011, **47**, 8650.
- 33 J. Oh, M. E. Kozlov, J. Carretero-Gonzalez, E. Castillo-Martinez and R. H. Baughman, *Chem. Phys. Lett.*, 2011, **505**, 31.
- 34 Y. F. Lian, Y. X. Liu, T. Jiang, J. Shu, H. Q. Lian and M. H. Cao, *J. Phys. Chem. C*, 2010, **114**, 9659.
- 35 D. Y. Lee, I. S. Park, M. H. Lee, K. J. Kim and S. Heo, *Sens. Actuators, A*, 2007, **133**, 117.
- 36 X. J. Xie, L. T. Qu, C. Zhou, Y. Li, J. Zhu, H. Bai, G. Q. Shi and L. M. Dai, *ACS Nano*, 2010, **4**, 6050.
- 37 X. X. Xie, X. H. Bai, G. Q. Shi and L. T. Qu, *J. Mater. Chem.*, 2011, **21**, 2057.
- 38 M. Hughes and G. M. Spinks, *Adv. Mater.*, 2005, **17**, 443.
- 39 J. H. Jung, J. H. Jeon, V. Sridhar and I. K. Oh, *Carbon*, 2011, **49**, 1279.
- 40 D. Cai and M. Song, *J. Mater. Chem.*, 2010, **20**, 7906.
- 41 O. C. Compton and S. T. Nguyen, *Small*, 2010, **6**, 711.
- 42 H. Bai, C. Li and G. Shi, *Adv. Mater.*, 2011, **23**, 1089.
- 43 Y. Zhu, S. Murali, W. Cai, X. Li, J. W. Suk, J. R. Potts and R. S. Ruoff, *Adv. Mater.*, 2010, **22**, 3906.
- 44 J. J. Liang, Y. F. Xu, D. Sui, L. Zhong, Y. Huang, Y. F. Ma, F. F. Li and Y. S. Chen, *J. Phys. Chem. C*, 2010, **114**, 17465.
- 45 J. J. Liang, Y. Huang, J. Y. Oh, M. Kozlov, D. Sui, S. L. Fang, R. H. Baughman, Y. F. Ma and Y. S. Chen, *Adv. Funct. Mater.*, 2011, **21**, 3778.
- 46 S. X. Lu and B. Panchapakesan, *Nanotechnology*, 2007, **18**, 305502.
- 47 H. Y. Jiang, S. Kelch and A. Lendlein, *Adv. Mater.*, 2006, **18**, 1471.
- 48 J. Cviklinski, A. R. Tajbakhsh and E. M. Terentjev, *Eur. Phys. J. E*, 2002, **9**, 427.
- 49 A. Lendlein, H. Y. Jiang, O. Junger and R. Langer, *Nature*, 2005, **434**, 879.
- 50 H. Koerner, G. Price, N. A. Pearce, M. Alexander and R. A. Vaia, *Nat. Mater.*, 2004, **3**, 115.
- 51 S. V. Ahir and E. M. Terentjev, *Nat. Mater.*, 2005, **4**, 491.
- 52 S. V. Ahir, A. M. Squires, A. R. Tajbakhsh and E. M. Terentjev, *Phys. Rev. B*, 2006, **73**, 085420.
- 53 L. Q. Yang, K. Setyowati, A. Li, S. Q. Gong and J. Chen, *Adv. Mater.*, 2008, **20**, 2271.
- 54 M. L. Auad, V. S. Contos, S. Nutt, M. I. Aranguren and N. E. Marcovich, *Polym. Int.*, 2008, **57**, 651.
- 55 A. Lendlein and S. Kelch, *Angew. Chem., Int. Ed.*, 2002, **41**, 2034.
- 56 F. K. Li, L. Y. Qi, J. P. Yang, M. Xu, X. L. Luo and D. Z. Ma, *J. Appl. Polym. Sci.*, 2000, **75**, 68.
- 57 H. Tobushi, H. Hara, E. Yamada and S. Hayashi, *Smart Mater. Struct.*, 1996, **5**, 483.
- 58 T. J. Booth, P. Blake, R. R. Nair, D. Jiang, E. W. Hill, U. Bangert, A. Bleloch, M. Gass, K. S. Novoselov, M. I. Katsnelson and A. K. Geim, *Nano Lett.*, 2008, **8**, 2442.
- 59 M. J. McAllister, J. L. Li, D. H. Adamson, H. C. Schniepp, A. A. Abdala, J. Liu, M. Herrera-Alonso, D. L. Milius, R. Car, R. K. Prud'homme and I. A. Aksay, *Chem. Mater.*, 2007, **19**, 4396.
- 60 C. Gomez-Navarro, R. T. Weitz, A. M. Bittner, M. Scolari, A. Mews, M. Burghard and K. Kern, *Nano Lett.*, 2007, **7**, 3499.
- 61 C. Gomez-Navarro, M. Burghard and K. Kern, *Nano Lett.*, 2008, **8**, 2045.
- 62 S. Stankovich, D. A. Dikin, G. H. B. Dommett, K. M. Kohlhaas, E. J. Zimney, E. A. Stach, R. D. Piner, S. T. Nguyen and R. S. Ruoff, *Nature*, 2006, **442**, 282.
- 63 T. Ramanathan, A. A. Abdala, S. Stankovich, D. A. Dikin, M. Herrera-Alonso, R. D. Piner, D. H. Adamson, H. C. Schniepp, X. Chen, R. S. Ruoff, S. T. Nguyen, I. A. Aksay, R. K. Prud'homme and L. C. Brinson, *Nat. Nanotechnol.*, 2008, **3**, 327.
- 64 C. G. Lee, X. D. Wei, J. W. Kysar and J. Hone, *Science*, 2008, **321**, 385.
- 65 H. A. Becerril, J. Mao, Z. Liu, R. M. Stoltenberg, Z. Bao and Y. Chen, *ACS Nano*, 2008, **2**, 463.
- 66 X. M. Sun, Z. Liu, K. Welscher, J. T. Robinson, A. Goodwin, S. Zaric and H. J. Dai, *Nano Res.*, 2008, **1**, 203.
- 67 Z. H. Fang, C. Punckt, E. Y. Leung, H. C. Schniepp and I. A. Aksay, *Appl. Opt.*, 2010, **49**, 6689.
- 68 S. Stankovich, R. D. Piner, S. T. Nguyen and R. S. Ruoff, *Carbon*, 2006, **44**, 3342.
- 69 S. Stankovich, D. A. Dikin, R. D. Piner, K. A. Kohlhaas, A. Kleinhammes, Y. Jia, Y. Wu, S. T. Nguyen and R. S. Ruoff, *Carbon*, 2007, **45**, 1558.
- 70 J. J. Liang, Y. F. Xu, Y. Huang, L. Zhang, Y. Wang, Y. F. Ma, F. F. Li, T. Y. Guo and Y. S. Chen, *J. Phys. Chem. C*, 2009, **113**, 9921.
- 71 S. Park, J. An, J. W. Suk and R. S. Ruoff, *Small*, 2010, **6**, 210.